Shahrood University of Technology

Iranian Society of Mining Engineering (IRSME)

Journal of Mining and Environment (JME)

journal homepage: www.jme.shahroodut.ac.ir

THOMSON REUTERS

Vol. 10, No. 2, 2019, 479-492.
DOI: 10.22044/jme.2019.7888.1654

# Study of convergence confinement method curves considering pore-pressure effect

K. Bour and K. Goshtasbi*

*Mining Engineering Department, Tarbiat Modares University, Tehran, Iran*

Received 23 December 2018; received in revised form 15 January 2019; accepted 19 January 2019

**Keywords**

*Convergence Confinement Method*

*Ground Reaction Curve*

*Longitudinal Deformation Profile*

*Strain Softening Behavior*

*Water*

**Abstract**

The design of underground spaces is mainly carried out using empirical, analytical, and numerical methods. The convergence confinement method (CCM) is an analytical technique that is widely utilized in analyzing the stability of underground spaces. However, the main challenge in the stability analysis is the selection of an accurate constitutive model for rock mass, and particularly, its post-failure behavior. The existence of water plays a significant role in the stability analysis, whereas this effect is not usually considered in the CCM method. In this research work, a circular tunnel in a saturated medium is modelled and compared with its dry condition. Two types of constitutive models namely elastic perfectly plastic (EPP) and strain softening (SS) are used and compared in order to investigate the effect of water and post-failure behavior on the stability of tunnels. With this respect, the codes are written and incorporated in the constitutive models and various analyses are carried out. The results achieved from the analyses show that the elastic reaction of ground in the presence of water in both constitutive models are the same and that the ground reaction curves (GRCs) and longitudinal deformation profiles (LDPs) are similar. However, the trend of GRC is different in the case where the rock failure occurs and the face of the tunnel goes beyond 0.5D. According to the results obtained, the maximum displacement in a saturated medium with different K values for the SS model is more than that for the EPP model.

**Nomenclature**

| | |
|---|---|
| GSI | Geological Strength Index |
| $p_0$ | Initial Stress |
| $p_i$ | Inner Pressure Acting on the Tunnel Boundary |
| $p_i^*$ | Critical Support Pressure |
| $p_i^{**}$ | Critical Pressure Between the Softening and Residual Zones |
| $K$ | Horizontal to Vertical *In Situ* Stress Ratio |
| $\eta$ | Softening Parameter (Plastic Shear Strain) |
| $\eta^*$ | Critical Softening Parameter |
| $E$ | Young's Modulus of Rock Mass |
| $c$ | Rock Mass Cohesion |
| $\varphi$ | Internal Friction Angle of Rock Mass |
| $\psi$ | Dilatancy Angle of Rock Mass |
| $\sigma_1$ | Maximum Principal Stress |
| $\sigma_3$ | Minimum Principal Stress |
| $\sigma_t$ | Tangential Stress |
| $\sigma_r$ | Radial Stress |
| $f$ | Failure Criterion |
| $g$ | Plastic Potential Function |
| $k_\psi$ | Dilation Coefficient |
| $k_\varphi$ | Friction Coefficient |

Corresponding author: goshtasb@modares.ac.ir (K. Goshtasbi Goharizi).

## 1. Introduction

In the design of underground structures, especially tunnels, stabilization of the surrounding rock mass is an important factor that must be considered [1]. Assessment of the support system required during the tunnel excavation and, in particular, in the nearby tunnel face is an essential issue. The Convergence Confinement Method (CCM) is a common tool for understanding the rock-support interaction problems. This method is widely used for the design of the support system for circular tunnels that are excavated in a variety of geological conditions [2].

The three main components of the CCM method are as follow:

1) Evaluation of tunnel deformation with respect to distance of the tunnel face, defined as the longitudinal deformation profile (LDP).

2) Correlation of the stress–strain in the support system identified as the support characteristic curve (SCC).

3) The ground reaction curve (GRC) can be defined as a curve that describes the decrease in inner pressure and the increase in radial displacement of the tunnel wall.

Corbeta et al. (1991) [3], Panet (1995) [4], and Unlu (2003) [5] have studied the LDP curve. These investigations were limited to the elastic constitutive model, and only the distance from the tunnel face and tunnel radius was considered as the input parameters. However, the results of the in-situ measurements, particularly in large deformation conditions, have shown that the elastic method is inaccurate [6]. Panet (1982) and Chern (1998) described a technique to obtain LDP for the Elastic Perfectly Plastic (EPP) constitutive model [7, 8]. In this technique, it is assumed that the tunnel is circular, the in-situ stresses are hydrostatic, and the input parameters are similar to the elastic constitutive model. Nejati et al have suggested a new formulation for calculation of LDP on the basis of rock mass quality [9]. On the other hand, Vlachopoulos and Diederichs (2009) have suggested a different solution for the EPP approach to estimate the LDP curve according to the ultimate plastic radius [2].

The method for obtaining the SCC curve was initially proposed for different types of supports by Hoek and Brown (1980) and then further discussed by Hoek (1999), CarranzaTorres and Fairhurst (2000), and Oreste (2003a,b, 2008) [10-15]. GRC, which describes the relationship between decrease in the inner support pressure and increase in the radial displacement of the tunnel wall, is generally evaluated by analytical elasto-plastic analyses and hydrostatic in-situ stresses [16-18].

As mentioned above, there exist adequate techniques to obtain CCM curves for tunnels excavated in elastic and perfectly plastic models and in a rock mass with a poor quality (GSI < 30). However, for all the other kinds of rock masses (GSI > 30) which show a strain-softening (SS) behavior, it seems that the problem has not been sufficiently analyzed. If failure occurs, none of these simple models adequately show the post-failure behavior of rock mass and especially the presence of water.

According to different inner pressures applied by the tunnel face and the support system after tunnel excavation, the surrounding rock mass based on the Strain-Softening (SS) behavior, three regions will be created as follow: elastic, softening, and residual. Each one of these regions can be seen in the GRC and LDP curves, which are used to determine the round length and stress relaxation (Figure 1). As it can be observed in this figure, by drawing a single line from E (the exact point behind the tunnel face describing the round length) to GRC, it will intercept it at point F. Then a line is drawn from F to the vertical axis ( $p_i$ ). From this interception to $p_0$ is called the stress relaxation.

In this work, we extended the CCM method to a circular tunnel excavated in a rock mass with an average quality (GSI = 30-75). The strain-Softening and Elastic Perfectly Plastic models in the FLAC code along the Mohr-Coulomb failure criterion were used to demonstrate the effects of water and constitutive model selection on the CCM curves. The SS model was developed by a FISH code in this research work.

## 2. Problem description

### 2.1. Strain-Softening constitutive model

It is common to use the EPP models to determine GRC [10, 19]. However, these plain models could not effectively characterize the real stress-strain behavior of rock masses in the occurrence of failure unless in rock masses with a low quality. Moreover, SS and elastic brittle models in the case of simulating the ground behavior are more appropriate for all other kinds of rock masses [19]. Based on other researcher's studies on post-failure behavior modes [20], the elastic perfectly plastic theory is not applicable to rock masses of average or high geotechnical quality (GSI of over 30). In other words, the EPP model is used in the rock

masses with a poor quality (GSI < 30). It is shown in Figure 2 that for rock masses with 75 < GSI < 90, the elastic brittle model could be suitable, and the SS model is more effective in terms of rock masses with 25 < GSI < 75 [19].

Regarding the progressive theory of plasticity to simulate, plastic deformation processes in which a material is described by a failure criterion $f$ and a plastic potential $g$, the SS behavior, stating the strength-weakening behavior, has been developed [21]. One of the main features of the SS model is that the failure criterion $f$ and the plastic potential $g$ depend on both the stress tensor and the plastic softening parameter $\eta$ [22]. Figure 3 illustrates the strength-weakening behavior for a confined compressive test; as it can be seen, M shows the slope of the softening step or drop modulus [19]. The perfectly brittle behavior occurs when this drop modulus has a tendency to infinity; in contrast, if it has a tendency to zero, the perfectly plastic behavior happens. With respect to the above-mentioned discussion, the SS model can be considered as a unique model including the elastic brittle plastic and the perfectly plastic behavior models. Accordingly, the elastic stage remains as long as the softening parameter is zero. The softening stage and the residual stage take place in $0<\eta<\eta^*$ and $\eta^*<\eta$, respectively. $\eta^*$ is defined as the critical value that establishes the change between the softening and residual stages [23].

In the softening stage, rock mass does not have its original strength properties, and reduction in the strength can be sensed. This reduction depends on the confinement stress ($\sigma_3$) and the softening parameter ($\eta$). Regarding the linear correlation among the strength properties ($c, \varphi, \psi$) and the softening parameter, the strength-weakening behavior of rock mass can be displayed (Figure 4).

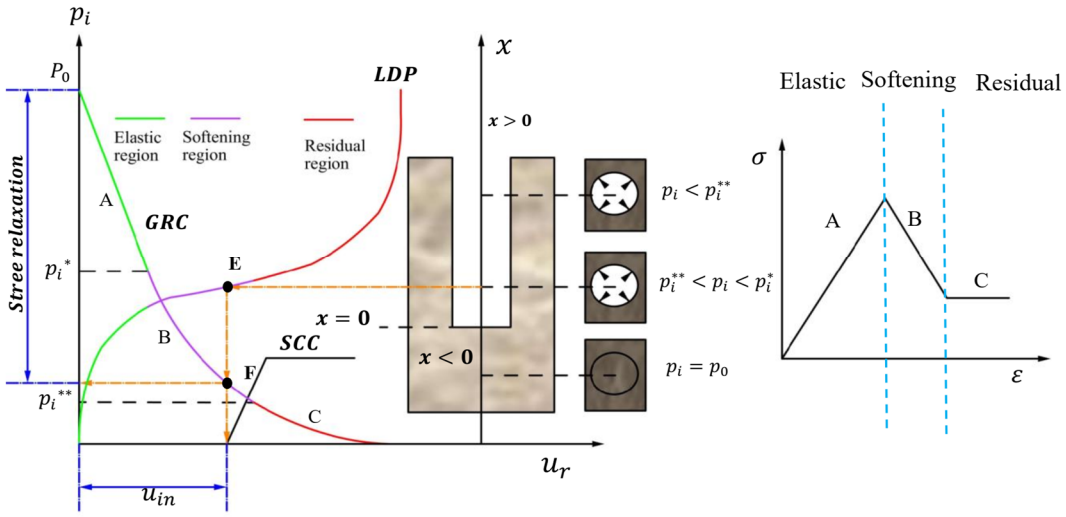


**Figure 1. The key elements of the CCM method.**

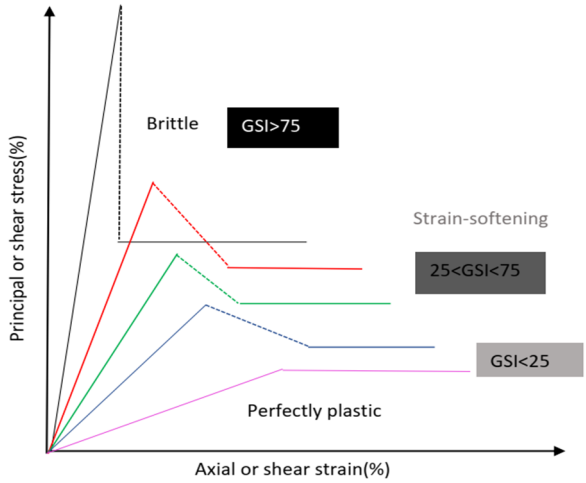


**Figure 2. Different post-failure modes in different GSI quantities [21].**

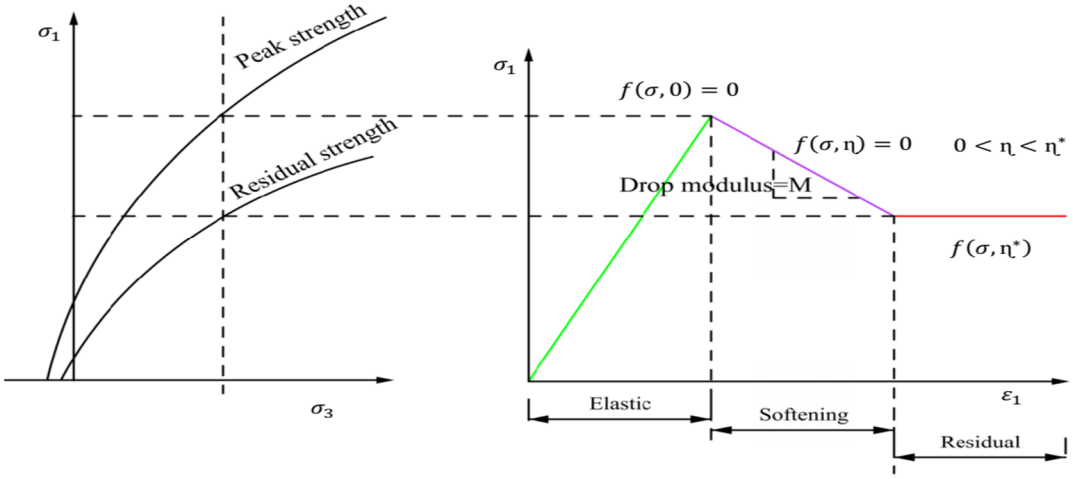


**Figure 3. Three different stages of a confined compressive test in a sample with a SS behavior [20].**

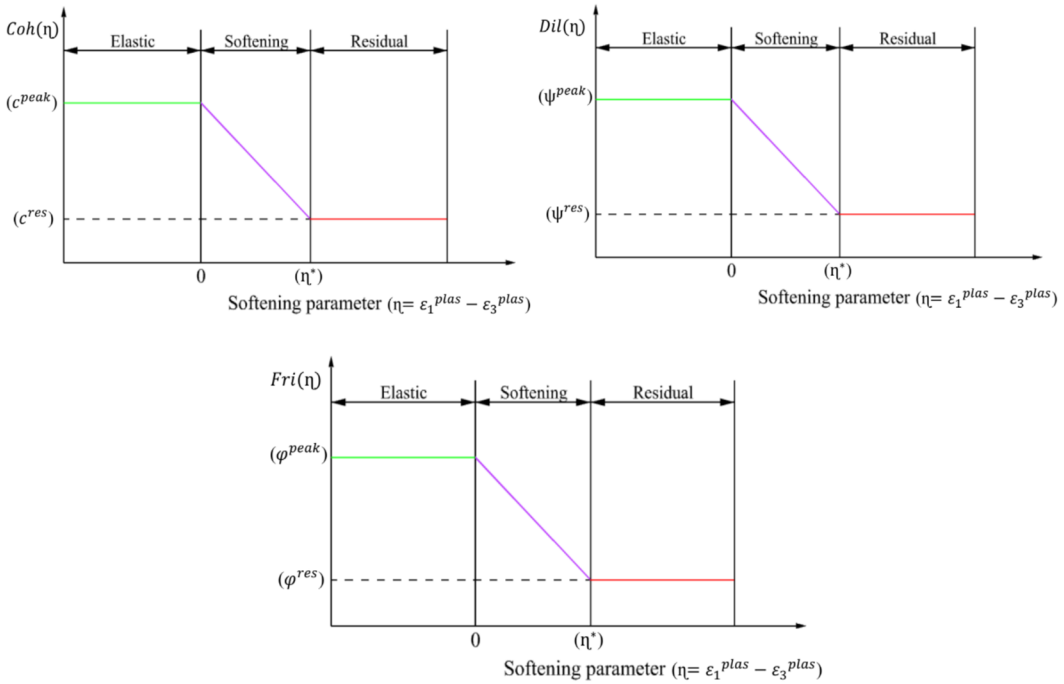


**Figure 4. The correlation among the strength properties and the softening parameter.**

### 2.2. Failure criterion and flow rule

In this work, the Mohr–Coulomb failure criterion as well as a plastic potential was used. These can be illustrated as follow [19]:

$$f(\sigma_r,\sigma_\theta,\eta)=$$
$$\sigma_\theta-k_\varphi(\eta)\sigma_r-2C(\eta)\sqrt{k_\varphi(\eta)} \quad (1)$$
$$\sigma_r=\sigma_3 \qquad \sigma_\theta=\sigma_1$$
$$g(\sigma_r,\sigma_\theta,\eta)=\sigma_\theta-k_\psi(\eta)\sigma_r \quad (2)$$

where $f$ is the failure criterion, $g$ is the plastic potential function, $\sigma_\theta$ is the tangential stress, and $\sigma_r$ is the radial stress. Besides, the dilation and friction coefficients are examined as follow [19]:

$$k_\psi(\eta)=\frac{1+\sin\psi(\eta)}{1-\sin\psi(\eta)} \quad (3)$$

$$k_\varphi(\eta)=\frac{1+\sin\varphi(\eta)}{1-\sin\varphi(\eta)} \quad (4)$$

If the plastic potential coincides with the failure criterion, then the rule is an associated flow rule; otherwise, it is termed as a non-associated flow rule. The parameters cohesion ($c$), friction angle ($\varphi$), and dilation angle ($\psi$) in association with the linear softening parameter function ($\eta$) are presented as follow [19]:

$$\varphi(\eta)=\begin{cases}\varphi^{peak}-\dfrac{\varphi^{peak}-\varphi^{res}}{\eta^{*}}\eta & 0<\eta<\eta^{*}\\ \varphi^{res} & \eta^{*}<\eta\end{cases} \quad (5)$$

$$c(\eta)=\begin{cases}c^{peak}-\dfrac{c^{peak}-c^{res}}{\eta^{*}}\eta & 0<\eta<\eta^{*}\\ c^{res} & \eta^{*}<\eta\end{cases} \quad (6)$$

$$\psi(\eta)=\begin{cases}\psi^{peak}-\dfrac{\psi^{peak}-\psi^{res}}{\eta^{*}}\eta & 0<\eta<\eta^{*}\\ \psi^{res} & \eta^{*}<\eta\end{cases} \quad (7)$$

and the softening parameter is the plastic shear strain:

$$\eta=\varepsilon_1^{p}-\varepsilon_3^{p}=\varepsilon_\theta^{p}-\varepsilon_r^{p}=\gamma^{p} \quad (8)$$

### 2.3. Development of SS code

Numerical methods have been developed because of the complexity occurring in the tunnel face through the excavation and the limitations of analytical methods to represent the CCM curves. To this end, the FISH code in the FLAC program was used to develop the SS behavior model. One of the main factors is to determine the critical softening parameter ( $\eta^{*}$ ) depending on the confinement stress ( $\sigma_3$ ). First, the quantity $\varepsilon_1^{plas}=\left[\sigma_1^{peak}(\sigma_3\right.$ with the assumed $\sigma_3$ was calculated, and then due to Figure 5 and the definition for Young's modulus and the drop modulus, the values $\varepsilon_1^{peak,elas}$ , $\varepsilon_1^{\Delta,drop}$ and $\varepsilon_1^{elas}$ can be calculated as follow [21]:

$$\varepsilon_1^{peak,elas}=\frac{\sigma_1^{peak}(\sigma_3)}{E} \quad (9)$$

$$\varepsilon_1^{\Delta,drop}=\frac{\left[\sigma_1^{peak}(\sigma_3)-\sigma_1^{res}(\sigma_3)\right]}{-M} \quad (10)$$

$$\varepsilon_1^{elas}=\frac{\sigma_1^{res}(\sigma_3)}{E} \quad (11)$$

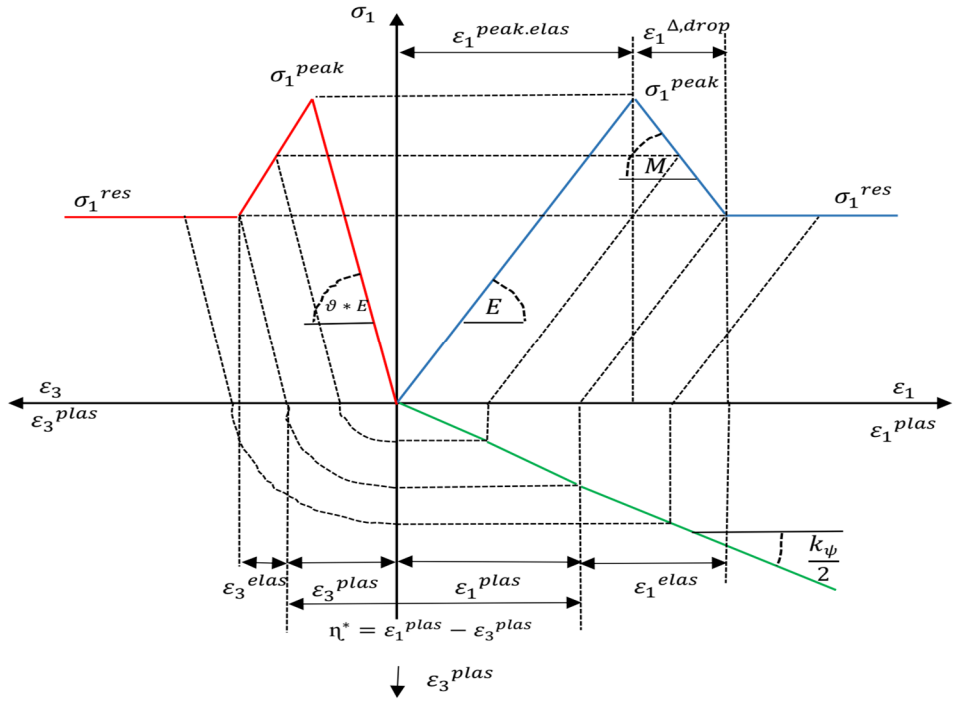


**Figure 5. Calculation of the critical softening parameter based on the stress-strain curve of rock [21].**

It is worth mentioning that the amount of M is considered as a negative value, and thus the amount of $\varepsilon_1^{\Delta,drop}$ is obtained as a positive value: $\frac{\left[\sigma_1^{peak}(\sigma_3)-\sigma_1^{res}(\sigma_3)\right]}{-M}$

$$\varepsilon_1^{plas}=\varepsilon_1^{peak,elas}+\varepsilon_1^{\Delta,drop}-\varepsilon_1^{elas} \quad (12)$$

$$\varepsilon_1^{plas}=\left[\sigma_1^{peak}(\sigma_3)-\left[\sigma_1^{res}(\sigma_3)\left[\frac{1}{E}-\frac{1}{M}\right]\right]\right] \quad (13)$$

$$\varepsilon_3^{plas}=-\frac{1}{2}\left(\frac{1+\sin\psi(\eta)}{1-\sin\psi(\eta)}\right)\varepsilon_1^{plas}=\frac{-k_\psi}{2}\varepsilon_1^{plas} \quad (14)$$

Hence, the critical softening parameter ($\eta^*$) for the assumed amount of ($\sigma_3$) can be gained as follows:

$$\eta^*(\sigma_3)=\varepsilon_1^{plas}-\varepsilon_3^{plas}= \left(1-\frac{E}{M}\right)\left(\frac{\sigma_1^{peak}(\sigma_3)-\sigma_1^{res}(\sigma_3)}{E}\right)\left(1+\frac{k_\psi}{2}\right) \quad (15)$$

It can be concluded that the critical softening parameter depends on both the confinement stress $\sigma_3$ and GSI [19]. As a result, the critical softening parameter can be estimated as follows:

$$\eta^*=\varepsilon_1^{plas}-\varepsilon_3^{plas}= \left(1-\frac{E}{M}\right)\left(\frac{\sigma_1^{peak}(\sigma_3)-\sigma_1^{res}(\sigma_3)}{E}\right)\left(1+\frac{k_\psi}{2}\right)= f_\eta(\sigma_3,GSI)\left(\frac{\sigma_1^{peak}(\sigma_3)-\sigma_1^{res}(\sigma_3)}{E}\right)\left(1+\frac{k_\psi}{2}\right) \quad (16)$$

Since the drop modulus is dependent upon the GSI and confinement stress $\sigma_3$, the critical softening parameter can be calculated as follows [19]:

$$f_\eta(\sigma_3,GSI)= \left[\left(\frac{225-GSI}{1000}\right)\sigma_3+\left(\frac{55-0.6GSI}{8}\right)\right] \quad (17)$$

for 25<GSI<75

### 2.4. Pore pressure effect

Early researchers have reported for rock masses with an average quality that the presence of water does not have a substantial influence on the strength and deformation of rocks; however, a confining pressure may decrease the water-weakening effect [24-26]. Then the effect of water has been considered as the decline in stress (Figure 6).

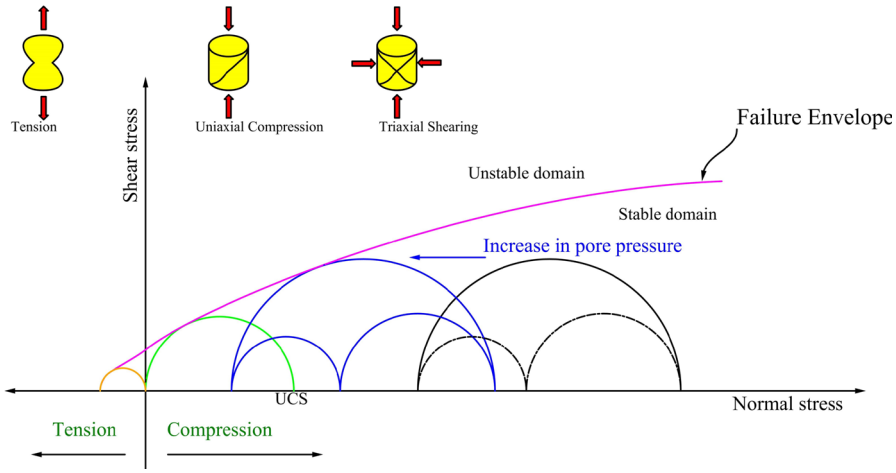


**Figure 6. The effect of water on rock failure.**

### 3. Verification of suggested correlations

The results of the experimental approach of granite specimens to verify the suggested correlations are used in this work [27]. The rate of height to diameter (h/d) and the diameter of specimens are considered as 2 mm and 54 mm, respectively. The results obtained are based upon 30 series of experimental tests regarding the confined pressure and unconfined pressure. Moreover, other types of tests such as the Brazilian test and the tilt test used to evaluate the mechanical properties of samples were conducted and the input results for the simulation can be seen in Table 1.

For verification of the suggested correlations, several tests of uniaxial and triaxial compression test were simulated ($\sigma_3$ = 2, 6, 10 MPa). The geometry and boundary condition of simulation is shown in Figure 7.

The results of the numerical and experimental tests are given in Figure 8. It can be seen that the peak and residual strengths of the samples for both the numerical and experimental approaches show a good consistency. With increase in the confining pressure, both the peak and residual strengths increase; however, the rate of growth for peak strength is more for the residual ones based upon Figure 8.

Furthermore, the effect of confining pressure on ductility of samples (reduction effect on drop modulus) can be sensed in the curves in Figure 8. In other words, the slope of the stress-strain curve in the softening region decreases with increase in the confined pressure; thus, the post peak behaviour of the samples shows a transition from a brittle type to a ductile one.

**Table 1. The mechanical parameters for simulation approach of granite samples [27].**

| Parameter | Density $\left(g/cm^3\right)$ | Elastic modulus (GPa) | Poisson' ratio | Cohesion (MPa) | Friction (°) | Dilation (°) | Tension (MPa) |
|---|---|---|---|---|---|---|---|
| Value | 2.61 | 18.97 | 0.19 | $c^{peak} = 12.42$<br>$c^{res} = 4.5$ | $\varphi^{peak} = 57.59$<br>$\varphi^{res} = 43.04$ | $\psi^{peak} = 50$<br>$\psi^{res} = 45$ | 6.65 |

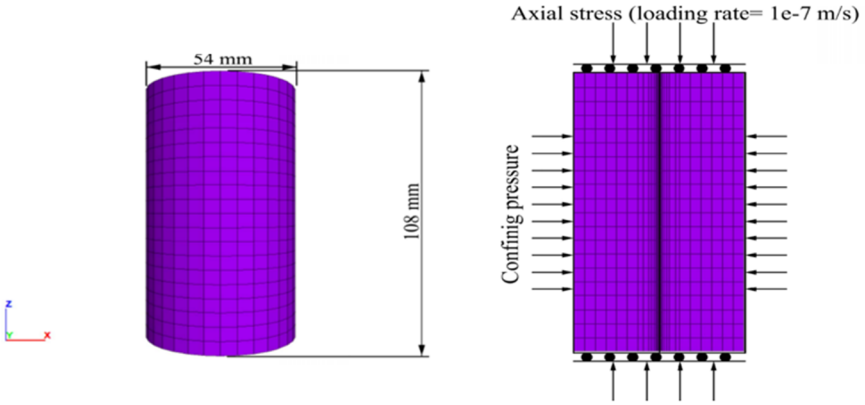


**Figure 7. The geometry and boundary conditions of samples for numerical approach.**

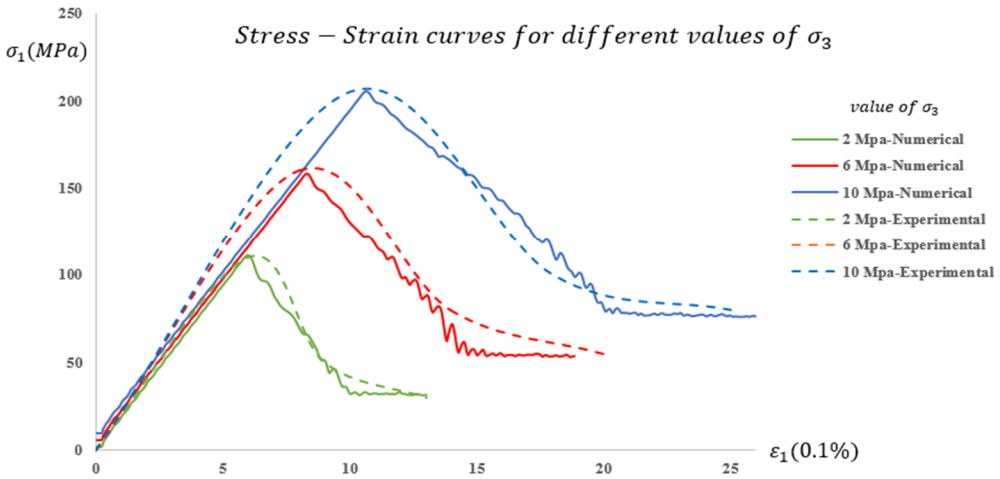


**Figure 8. The comparison of strain-stress curves of numerical and experimental approaches for different confining pressures.**

## 4. Application of CCM method

### 4.1. Numerical approaches

In the case of average quality of rocks, a basaltic rock mass was selected and studied based upon [19]. They have reported an average unconfined compressive strength, and mi as 23 MPa and 10, respectively. Also the GSI value was estimated to be 55, the Barton's Q value was obtained to be between 1 and 5, and the residual GSI value was calculated as 33 [19]. Due to introduction of this rock mass in the RocLab program [28], the results are shown in Table 2. The porosity value was considered to be 0.33.

Tunnels measured 7 m in diameter and 450 m in depth in the saturated surrounding were selected and modelled. A slightly larger discretized area of 70 m * 70 m * 28 m was selected, and the tunnels were located 4 to 5 times of the tunnel diameter far from the boundaries. The surrounding environment in modelling was considered as the isotropic material and the rock mass behaviour, assumed as EPP and SS through the Mohr-Coulomb failure criterion. The mesh size was regularly reduced near the tunnel zone. The increase in the number of nodes could enhance the accuracy of calculation. To this end, two different simulations with different total number of elements 19600 and 132472 were used in FLAC 2D and 3D [29, 30], respectively (Figure 9).

**Table 2. Rock mass geological parameters [19].**

| Parameter | Unit | Value |
|---|---|---|
| $GSI^{peak}$ | | 55.0 |
| Q | | 1-5 |
| $GSI^{res}$ | | 33.0 |
| $\sigma_{ci}$ | MPa | 23 |
| $m_i$ | | 10 |
| $\gamma$ | $KN/m^3$ | 26.70 |
| E | GPa | 3.837 |
| Θ | | 0.25 |
| $c^{peak}$ | MPa | 0.744 |
| $\varphi^{peak}$ | ° | 24.81 |
| $\psi^{peak}$ | ° | 3.72 |
| $c^{res}$ | MPa | 0.397 |
| $\varphi^{res}$ | ° | 15.69 |
| $\psi^{res}$ | ° | 0 |
| $\psi^{peak,res} = \frac{5GSI^{peak,res} - 125}{1000}\varphi$ | | for $25 < GSI < 75$ |

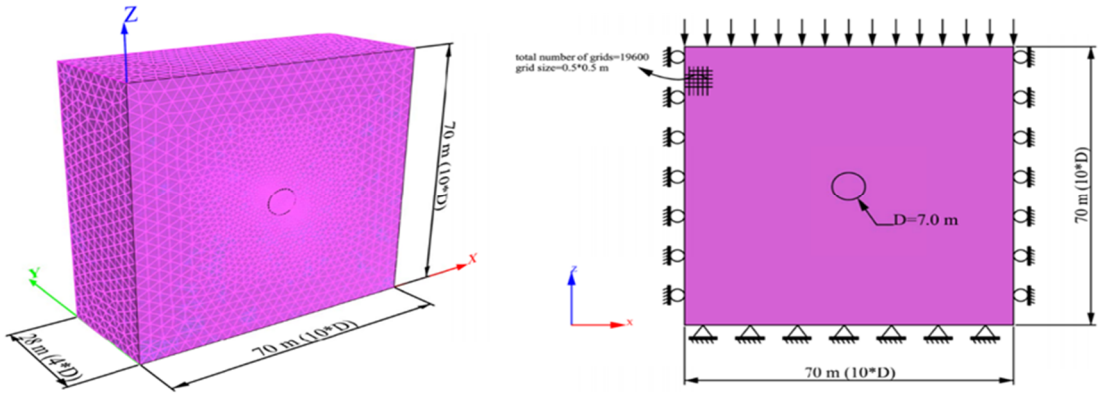


**Figure 9. Geometry and meshes used for numerical modeling in both (a) 2D and (b) 3D approaches.**

### 4.2. Ground reaction curve (GRC)

GRC is used to show the correlation between the surrounding materials in which a tunnel is excavated and the support system. If the pressure of the support system is as the exact amount of the in-situ stress pressure on tunnel walls after excavation, there will be no difference in the stress conditions after and before excavation. Consequently, no displacement will occur in this case. By gradually reducing the pressure of the support system, displacements associated with every single step of pressure reduction can be calculated. The maximum displacement occurring in terms of the pressure of support system tends to be zero. GRCs for two different circumstances of dry and saturated environment with EPP and SS behaviours in three diverse amounts of K (0.5, 1, and 1.5) based on the aforementioned discussions were represented by FLAC 2D.

Figure 10 shows GRCs for k = 0.5 in both the dry and saturated environments associated with the EPP and SS constitutive models. It can be seen that in the existence of water, the displacements increase and the maximum displacement in the EPP model in dry condition is altered by 65 mm to 360 mm in the saturated ones. The alteration of displacement in

the SS model was obtained as 330 mm to 580 mm for dry and saturated conditions, respectively. Moreover, the elastic reaction curves for both conditions (dry and saturated) were similar. In other word, the critical pressure ( $p_i^*$ ) between the elastic and plastic zones will be 60-70% of the in-situ stresses but the distinct differences between GRCs can be sensed about the 70% of stress relaxation. However, the critical pressure between the softening and residual zones ( $p_i^{**}$ ) will be 20-30% of the in-situ stresses.

GRCs for k =1 in both the dry and saturated environments associated with the EPP and SS constitutive models are shown in Figure 11. In the existence of water, the displacements rise, like previously. The maximum displacement in the EPP model in the dry condition was altered by 100 mm to 400 mm in the saturated one. This change of displacement in the SS model was gained as 530 mm and 710 mm for the dry and saturated conditions, respectively. It could be seen that GRCs were similar up to 60% of stress relaxation. Thus it can be concluded that the critical pressure ( $p_i^*$ ) between the two regions (elastic and plastic) in this situation will be 40% of the in-situ stresses.

GRCs for k = 1.5 in both the dry and saturated environments associated with the EPP and SS constitutive models are shown in Figure 12. In this case, the maximum displacement in the EPP model in the dry condition changed by 240 mm to 480 mm in the saturated one. This alteration of displacement in the SS model was gained as 940 mm and 1330 mm for the dry and saturated conditions, respectively. It could be seen that GRCs were alike up to 50% of stress relaxation. Accordingly, it can be concluded that the critical pressure ( $p_i^*$ ) between the two regions (elastic and plastic) in this situation will be 50% of the in-situ stresses.

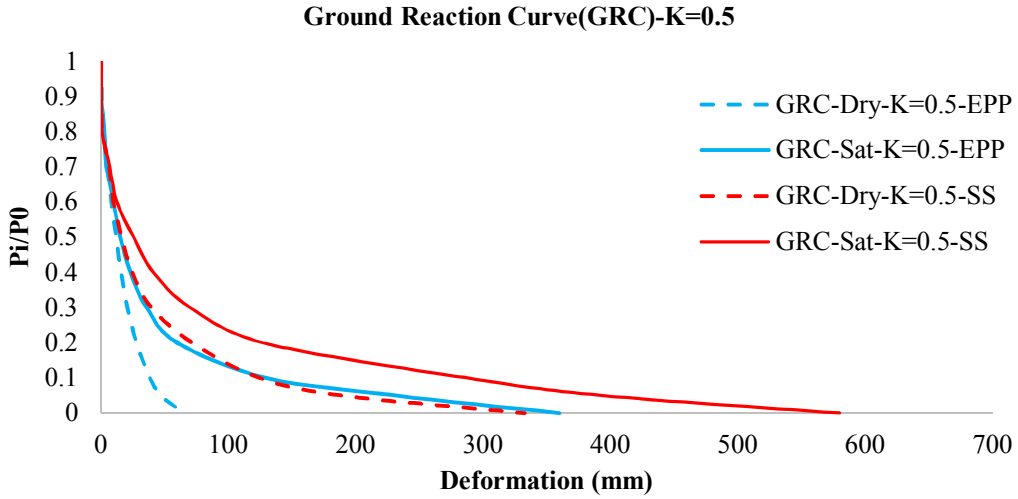


**Figure 10. GRCs in two conditions (dry and saturated) for k = 0.5.**

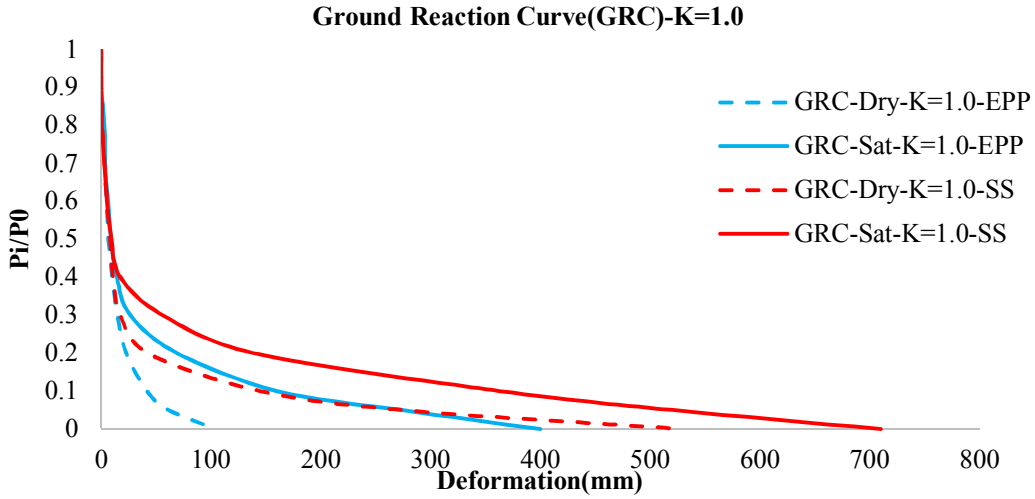


**Figure 11. GRCs in two conditions (dry and saturated) for k = 1.**

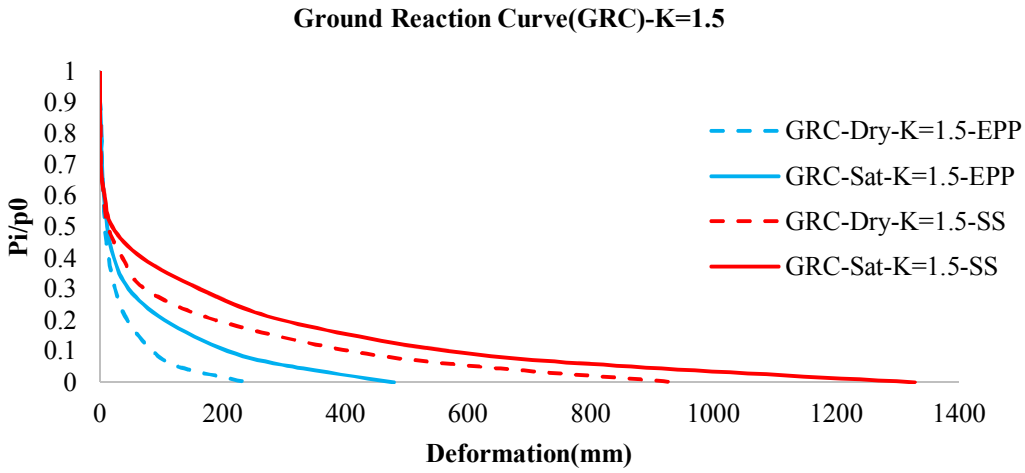


**Figure 12. GRCs in two conditions (dry and saturated) for k = 1.5.**

It is worth mentioning that the results of the EPP constitutive model in the saturated condition could not represent the accurate effect of water. As it can be seen, in all different conditions (Figures 10-12) through different K values, the maximum displacements are very similar to each other (360, 400, 480 mm). Nevertheless, in the SS constitutive model, for different K values, displacement differences were obtained in the presence of water (580, 710, 1330 mm).

### 4.3. Longitudinal deformation profile (LDP)

A single longitudinal section of an excavated tunnel can be divided into three regions: (a) ahead of the face, (b) the face, and (c) behind the face. Conditions of stresses in front of the face are similar to the in-situ stresses. On the other hand, stress conditions are distributed in the face as though the effect of face supporting on the tunnel wall can be seen. Finally, there is no confinement influence on the face behind, and the maximum displacements would happen. Like Figure 13, if point A in an excavated tunnel on the tunnel roof is taken into account, the radial displacements extremely depend upon both the strength and mechanical properties of rock mass. By closing the face of tunnel to the mentioned point (A), the radial confinement pressure would reduce.
Furthermore, the displacements steadily increase in the case that the face of the tunnel and point A have an extensive distance because the effects of the tunnel face and the confinement pressure reduce (Figure 14).

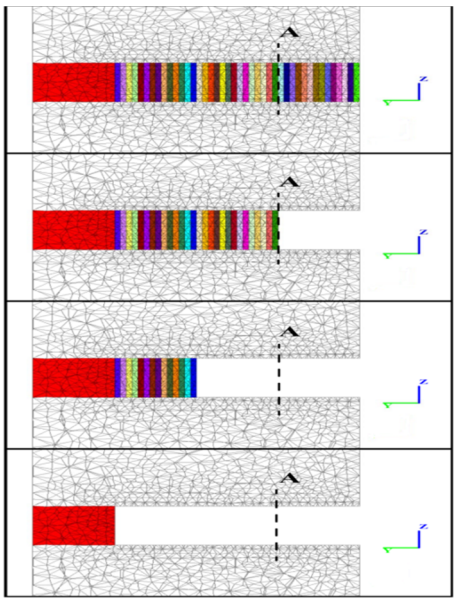


**Figure 13. The position of A remark to determine LDP.**

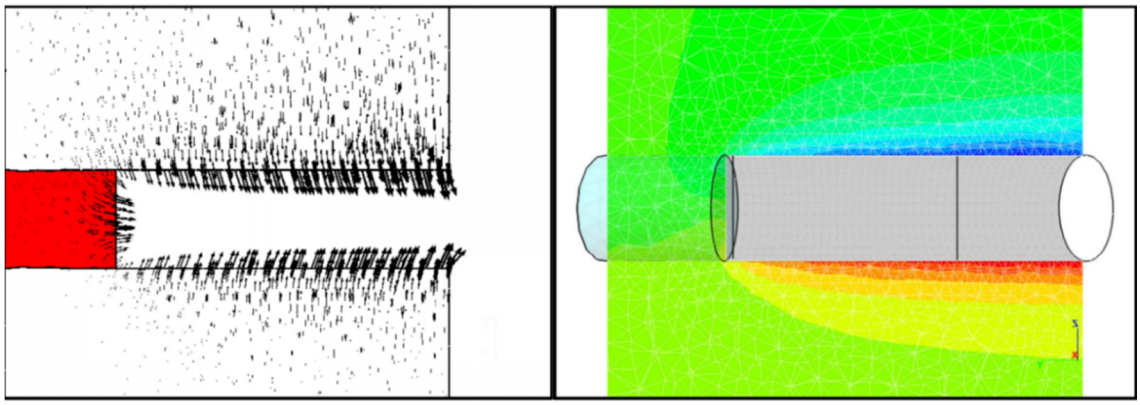

**Figure 14. The radial displacement of the excavated tunnel.**

Figure 15 shows LDPs for k = 0.5 in both the dry and saturated environments associated with the EPP and SS constitutive models. As it can be seen in this figure and the previous GRC figures, the maximum displacements are similar, implying the accuracy of the numerical simulation. The difference between the results of the dry and saturated conditions in both models are worth mentioning. These alterations commence from the face of the tunnel to behind it. For instance, the displacement at the tunnel face for the EPP and SS models in the dry condition was obtained to be 23 mm and 128 mm, respectively.

The displacements at the tunnel face in the existence of water for both constitutive models are the same. However, the differences can be sensed behind the tunnel face at the 0.5D distance. In other words, these variances show more alterations by moving the tunnel face advance because of the reduction in the confinement pressure and the effect of the tunnel face supporting pressure.

LDPs in different conditions (dry and saturated) associated with the EPP and SS constitutive models for K = 1 are shown in Figure 16. The alterations between the constitutive models commence from the face of the tunnel to behind it. For example, the displacement at the tunnel face for the EPP and SS models in the dry condition was gained to be 27 mm and 176 mm, respectively.

LDPs in different conditions (dry and saturated) associated with the EPP and SS constitutive models for K = 1.5 can be seen in Figure 17. The differences of constitutive models were less in this circumstance in comparison to the two previous K values. For instance, the displacement at the tunnel face for the EPP and SS models in the dry condition was gained to be 34 mm and 138 mm, respectively.

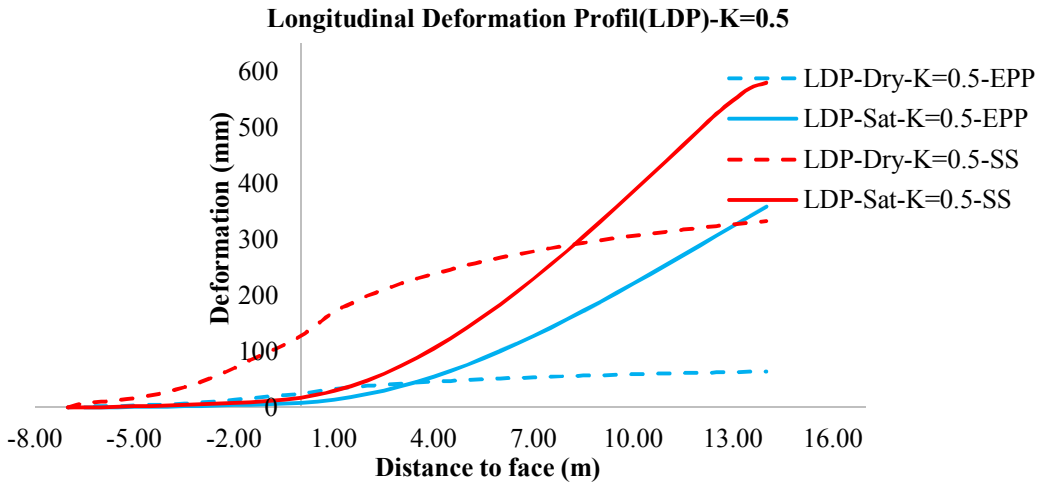


**Figure 15. LDPs in two conditions (dry and saturated) for k = 0.5.**

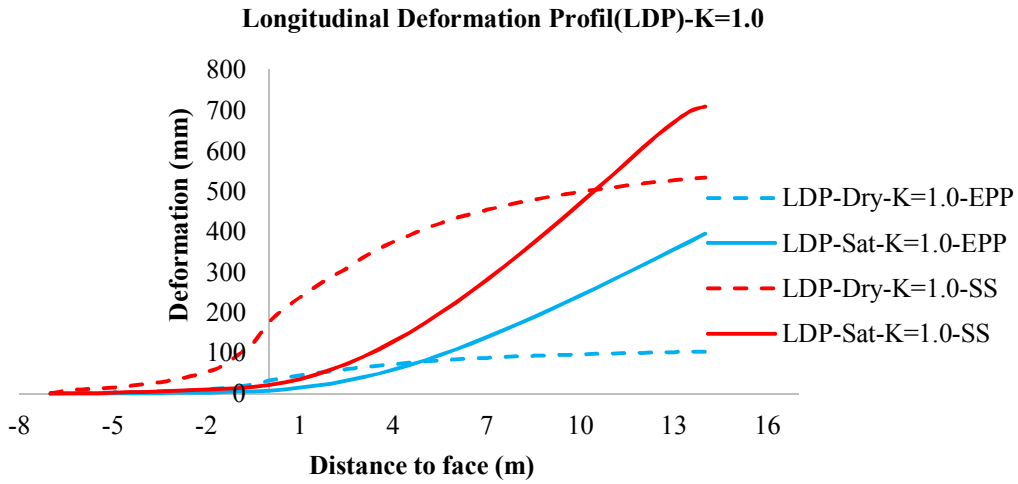


**Figure 16. LDPs in two conditions (dry and saturated) for k = 1.**

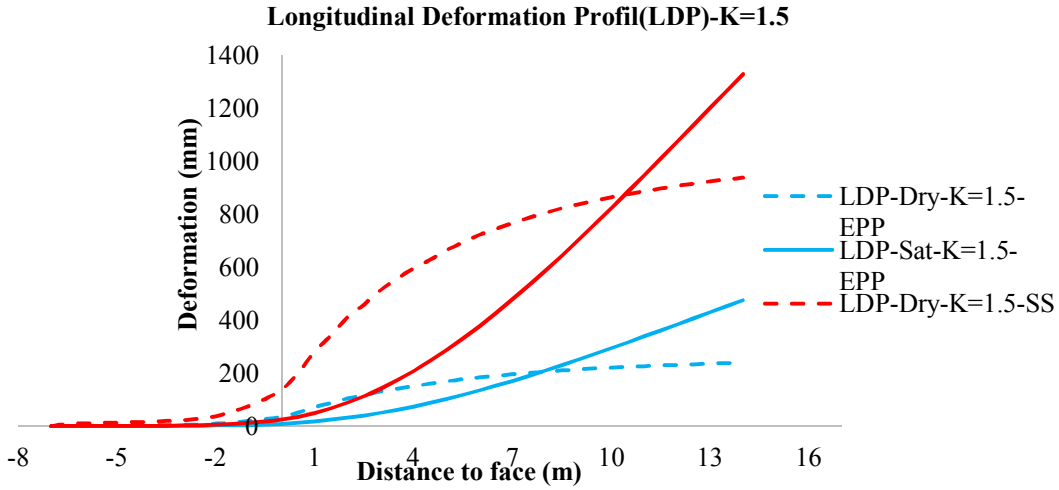


**Figure 17. LDPs in two conditions of dry and saturated for k=1.5.**

## 5. Conclusions

The main reasons for the immense differences among the CCM curves based on the analytical and numerical methods is the incorrect selection of the constitutive model and simple assumptions and limitations that do not coincide with reality. Likewise, the use of SS model and consideration of water are the additional difficulties. In this research work, the reaction of the ground around the circular tunnel excavated in both the saturated and dry media with different K values (0.5, 1, and 1.5) were analysed by the numerical approach. Furthermore, the impacts of the different models (EPP and SS) on GRCs and LDPs were successfully analysed in the FLAC 2D and 3D code. The aim of these methods is to overcome the limitations described above.

The results of the analyses show that there is a considerable difference between LDPs and GRCs in both the saturated and dry condition utilizing two constitutive models. The GRC and LDP curves in the presence of water in the elastic region are the same for both constitutive models. However, when the rock mass is broken and enters the post-peak region, the difference between the curves begins, and this difference increases with the face advance. This difference in the saturated condition is started about 0.5D behind the face for both constitutive models, and will be increased as the face advances. The maximum displacement in a saturated medium with different K values for the EPP model is less than that of the SS model. This is due to the fact that in the post-failure region, the strength parameters in the EEP model is constant, whereas in the SS model, the strength-weakening effect is considered. Furthermore, the presence of water makes the GRC and LDP curves deviate more in the EEP model in comparison to the SS model.

## References

[1]. Guan, Z., Jiang, Y. and Tanabasi, Y. (2007).

Ground reaction analyses in conventional tunnelling excavation. Tunnelling and Underground Space Technology. 22 (2): 230-237.

[2]. Vlachopoulos, N. and Diederichs, M.S. (2009). Improved longitudinal displacement profiles for convergence confinement analysis of deep tunnels. Rock Mechanics and Rock Engineering. 42 (2): 131-146.

[3]. Corbetta, F., Bernaud, D. and Nguyen-Minh, D. (1991). Contribution a la methode convergence-confinement par le principle de la similitude. Rev. Fr. Geotech. 54: 5-11.

[4]. Panet, M. (1995). Calcul des Tunnels par la Methode de Convergence-Confinement. Presses de l'Ecole Nationale des Ponts et Chausse'es, Paris. 178 P.

[5]. Unlu, T. and Gercek, H. (2003). Effect of Poisson's ratio on the normalized radial displacementsoccurring around the face of a circular tunnel. Tunnelling and Underground Space Technology. 18 (5): 547-553.

[6]. Alejano, L.R., Rodriguez-Dono, A. and Veiga, M. (2012). Plastic radii and longitudinal deformation profiles of tunnels excavated in strain-softening rock masses. Tunnelling and Underground Space Technology. 30: 169-182.

[7]. Panet, M. and Guenot, A. (1982). Analysis of convergence behind the face of a tunnel. Proceedings of the International Symposium Tunnelling, IMM, London, UK.

[8]. Chern, J.C., Shiao, F.Y. and Yu, C.W. (1998). An empirical safety criterion for tunnel construction, Proceedings of the Regional Symposium on Sedimentary Rock Engineering, Taipei, Taiwan, November.

[9]. Rooh, A., Nejati, H.R. and Goshtasbi, K. (2018). A new formulation for calculation of longitudinal displacement profile (LDP) on the basis of rock mass quality. Geomechanics and Engineering. 16 (5): 539-545.

[10]. Hoek, E. and Brown, E.T. (1980). Underground Excavations In Rock. The Institution of Mining and Metallurgy, London. UK.

[11]. Hoek, E. (1999). Support for very weak rock associated with faults and shear zones. International Symposium on Rock Support and Reinforcement Practice in Mining, Kalgoorlie, Australia, March.

[12]. Carranza-Torres, C. and Fairhurst, C. (2000). Application of the convergence-confinement method of tunnel design to rock masses that satisfy the Hoek-Brown failure criteria. Tunnelling and Underground Space Technology. 15 (2): 187-213.

[13]. Oreste, P. (2003). Analysis of structural interaction in tunnels using the convergence–confinement approach. Tunnelling and Underground Space Technology. 18 (4): 347-363.

[14]. Oreste, P. (2003). A procedure for determining the reaction curve of shotcrete lining considering transient conditions. Rock Mechanics and Rock Engineering. 36 (3): 209-236.

[15]. Oreste, P. (2008). Distinct analysis of fully grouted bolts around a circular tunnel considering the congruence of displacements between the bar and the rock. International Journal of Rock Mechanics and Mining Sciences. 45 (7): 1052-1067.

[16]. Hoek, E., Carranza-Torres, C., Diederichs, M.S. and Corkum, B. (2008). Kersten Lecture Integration of geotechnical and structural design in tunneling. 56th Annual Geotechnical Engineering Conference, University of Minnesota, USA, February.

[17]. Molladavoodi, H. (2013). Study of ground response curve (GRC) based on a damage model. Archives of Mining Sciences. 58 (3): 655-672.

[18]. Lazemi, H.A., Fatehi Marji, M., Yarahmadi Bafghi, A.R. and Goshtasbi, K. (2013). Rock failure analysis of the broken zone around a circular opening. Archives of Mining Sciences. 58 (1): 165-188.

[19]. Alejano, L.R., Rodriguez-Dono, A., Alonso, E. and Fdez-Manin, G. (2009). Ground reaction curves for tunnels excavated in different quality rock masses showing several types of post-failure behavior. Tunnelling and Underground Space Technology. 24 (6): 689-705.

[20]. Hoek, E. and Brown, E.T. (1997). Practical estimates of rock mass strength. International Journal of Rock Mechanics and Mining Sciences. 34 (8): 1165-1186.

[21]. Alejano, L.R., Alonso, E., Rodriguez-Dono, A., and Fdez-Manin, G. (2010). Application of the convergence-confinement method to tunnels in rock masses exhibiting Hoek–Brown strain-softening behavior. International Journal of Rock Mechanics & Mining Sciences. 47 (1): 150-160.

[22]. Cui, L., Zheng, J.J., Zhang, R.J. and Lai, H.J. (2015). A numerical procedure for the fictitious support pressure in the application of the convergence–confinement method for circular tunnel design. International Journal of Rock Mechanics & Mining Sciences. 78: 336-349.

[23]. Alonso, E., Alejano, L.R., Varas, F., Fdez-Manin, G. and Carranza-Torres, C. (2003). Ground response curves for rock masses exhibiting strain-softening behavior. International Journal for Numerical and Analytical Methods in Geomechanics. 27 (13): 1153-1185.

[24]. Zhou, H., Zhang, C., Li, Z., Hu, D. and Hou, J. (2014). Analysis of mechanical behavior of soft rocks and stability control in deep tunnels. International Journal of Rock Mechanics and Mining Sciences. 6 (3):

219-226.

[25]. Wang, S.R., Hagan, P., Li, Y.C., Zhang, C.G. and Liu, X.L. (2017). Experimental Study on Deformation and Strength Characteristics of Sandstone with Different Water Contents. Journal of Engineering Science and Technology Review. 10 (4): 199-203.

[26]. Javadi, M. and Sharifzadeh, M. (2017). Groundwater and Underground Excavations: from Theory to Practice. Rock Mechanics and Engineering. 3: 299-330.

[27]. Arzúa, J. and Alejano, L.R. (2013). Dilation in granite during servo-controlled triaxial strength tests. International Journal of Rock Mechanics & Mining Sciences. 61: 43-56.

[28]. Rocscience. (2002). RocLab, https://www.rocscience.com.

[29]. Itasca, FLAC 2D Version 8.0. (2016). https://www.itascacg.com

[30]. Itasca, FLAC 3D Version 5.01 (2013). https://www.itascacg.com

# اثر آب بر روی منحنی‌های همگرایی- محدودیت

**کمیل بور و کامران گشتاسبی***

**بخش مهندسی معدن، دانشگاه تربیت مدرس، ایران**

ارسال ۲۰۱۸/۱۲/۲۳، پذیرش ۲۰۱۹/۱/۱۹

* نویسنده مسئول مکاتبات: goshtasb@modares.ac.ir

**چکیده:**

اکثر طراحی سازه‌های زیرزمینی بر اساس روش‌های تجربی، تحلیلی و عددی می‌باشند. روش همگرائی- محدودیت (CCM) یکی از تکنیک‌های تحلیلی است که به طور گسترده‌ای برای تحلیل پایداری سازه‌های زیرزمینی استفاده می‌شود. انتخاب مدل رفتاری صحیح برای توده سنگ و به ویژه رفتار بعد از شکست آن، یکی از چالش‌های مهم در آنالیز پایداری سازه‌های زیرزمینی است. در کلیه روابط ارائه شده برای روش CCM، مسئله حضور آب لحاظ نشده، در حالی که حضور آب به عنوان یک فاکتور کلیدی در طراحی تونل همیشه مطرح است. در این پژوهش از اطلاعات یک تونل با شکل مقطع دایروی و در دو شرایط خشک و اشباع، برای مقایسه استفاده شده است. برای مطالعه تأثیر انتخاب مدل رفتاری و اثر آب، از مدل‌های رفتاری الاستو پلاستیک کامل (EPP) و کرنش نرم شونده (SS) برای آنالیز عددی و مقایسه بین نتایج، استفاده شده است. با انجام آنالیز مشاهده شد که پاسخ الاستیک زمین در شرایط حضور آب، برای هر دو مدل رفتاری یکسان است و منحنی‌های GRC و LDP بر روی یکدیگر قرار می‌گیرند. اما با شکست توده سنگ اختلاف بین این منحنی‌ها بیشتر شده و زمانی که جبهه کار به اندازه نصف قطر تونل (0.5D) دور می‌شود، به این اختلافات افزوده خواهد شد. همچنین بیشینه جابجایی در شرایط مختلف K و در حالت آبدار، بیشتر از حالت خشک بوده، اما اختلاف بین آن‌ها برای مدل رفتاری EPP اندک بوده و برای مدل رفتاری SS کاملاً محسوس می‌باشد.

**کلمات کلیدی:** روش همگرایی- محدودیت، منحنی پاسخ زمین، پروفیل تغییر شکل طولی تونل، مدل رفتاری کرنش نرم شونده، آب.